Three-axis force visualizing system for fiberscopes utilizing highly elastic fabric

メタデータ	言語: eng
	出版者:
	公開日: 2017-10-03
	キーワード (Ja):
	キーワード (En):
	作成者:
	メールアドレス:
	所属:
URL	https://doi.org/10.24517/00009563

Three-axis force visualizing system for fiberscopes utilizing highly elastic fabric

Takanobu Iwai, Yoshinori Fujihira, Lina Wakako, Hiroyuki Kagawa, Takeshi Yoneyama, and Tetsuyou Watanabe, *Member, IEEE*

Abstract—**This paper presents a novel force sensing system for fiberscopes. The key features of the system are its low cost, high resolution, small size, and ability to measure three-dimensional force. A previous study described a novel force sensing system that could be attached to a very thin fiberscope, based on a force visualization mechanism utilizing panty stocking fabric—a highly elastic material. However, this system measures force in only one direction. In this paper, the system is extended to measure forces in any of three directions. The system is targeted for application to neurosurgical examinations. It may also be useful for other medical and non-medical examinations that involve the use of fiberscopes.**

I. INTRODUCTION

Fiberscopes and endoscopes are widely used to examine areas where humans cannot see directly. They are commonly used for medical examinations, although they can also be used for industrial examinations. However, only visual information can be obtained with current systems. If tactile information could be obtained, the examinations would be more valuable. In particular, tactile/force information is important when the visible area is limited. A typical example occurs in neurosurgery, where the doctor is required to treat tumors that are seated deeply within the brain and surrounded by healthy tissues. Considering this issue, a force sensor system that could be attached to the tip of an endoscope [1] was previously developed. However, this system measures the force only in one direction. This paper presents an extended version of the aforementioned force sensing system that can measure three-dimensional forces.

Many force and tactile sensors have been developed for medical instruments. Puangmali et al. [2] reviewed research on force and tactile sensors for minimally invasive surgery. The purpose of force sensing is to provide feedback to the operator on the sensation of touching an organ (see [3]–[6] for reviews). Most force sensors that have been developed include electric devices such as strain gauges. However, electrical devices are not always suitable for medical devices. Electrical force sensors require amplifiers, and the size and cost of the overall system becomes large. Electrical sensors also require wiring for signal transfer, although wiring easily causes noise. In addition, sterilizing or disinfecting such electrical devices is difficult. One solution to these issues is to build a system without using electrical parts. Takaki et al. [7] developed a force sensor based on force visualization by using moiré fringe patterns. Tadano and Kawashima [8] developed a system to

generate feedback on force sensation without a force sensor by utilizing a pneumatic servo system. Kawahara et al. [9] developed a system to measure the stiffness of an organ by pushing it with air and capturing its deformation by using a camera. Peirs et al. [10] developed a force sensor that detects the deformation of a flexible structure by using optical fibers. Tada et al. [11] developed a force sensor that functions in MRI environments by detecting, via photo-sensors, changes in the peak illumination of a point light source attached to the tip of an elastic frame. These sensors are mainly used for laparoscopic surgery, in which the part size and forces measured are larger (in the cm and N ranges, respectively) than the corresponding values that would be ideal for endoscopy in neurosurgery (in the mm and mN ranges). Sensors utilizing force visualization have been developed, although their intended applications are not medical. Ohka et al. [12] have developed a three-axis force sensor by observing the states of conical feelers with a camera. Kamiyama et al. [13] have developed a sensor that measures the direction, magnitude, and distribution of force by observing two layers of spherical markers with a camera. However, applying these concepts to force sensors in small and thin fiberscopes requires that the sensor size be reduced and a method to construct small markers be developed. In general, this issue is considered the disadvantage of sensors utilizing force visualization, as noted in previous studies [6], [14]. In contrast, a robotic system with a force sensor and feedback systems for neurosurgery was developed in [15]–[17]. However, because the force sensing system was based on a strain gauge, the aforementioned issues of sterilization and MRI compatibility were not resolved.

Considering these issues, a force sensing system based on force visualization, which can be attached to a fiberscope, was developed in this study. The key features of the proposed force sensing system are as follows.

Force visualization mechanism utilizing a highly elastic panty stocking fabric: To ensure both small size and high resolution, panty stocking fabric (shown in Fig. 1) is used for detecting force. The fabric is highly elastic and can deform even if the applied force is extremely small. In addition, the material is thin, inexpensive, and lightweight. A force visualization approach that utilizes this fabric was adopted because visual information could be obtained through fiberscopes, and only a force-detecting component is needed

T. Iwai and Y. Fujihira are with the Department of mechanical Engineering, College of science and engineering, Kanazawa University, Ishikawa, Japan (corresponding author to provide e-mail: iwai.t@stu.kanazawa-u.ac.jp).

L. Wakako, H. Kagawa, T. Yoneyama, and T. Watanabe are with School of Mechanical Engineering, College of Science and Engineering, Kanazawa University, Ishikawa, Japan (e-mail: linawakako@se.kanazawa-u.ac.jp; kagawa@t.kanazawa-u.ac.jp; yoneyama@t.kanazawa-u.ac.jp; te-watanabe@ieee.org).

to construct the force sensor. Hence, the force sensing system can be produced at a very low cost.

Figure 1. Panty stocking fabric

High resolution and small size: Owing to the high elasticity of the stocking fabric, a resolution of more than 0.015 [N] is realized. The part for detecting force is extremely compact, and its diameter is less than 3 [mm]. It does not include electrical components; therefore, sterilization is simple and MRI-compatibility easy to achieve. In addition, the part is disposable and its manufacturing cost is low.

II. FORCE DETECTING PART

A. Target situation

In this paper, the situation where a medical doctor examines a candidate tumor area by touching or nudging it with the developed sensor to identify the affected area precisely, while observing the area with other endoscopes is considered. The examination is normally performed by applying pressure to tissues, and rarely involves their release from pressure. Therefore, the focus of this paper is on applying pressure to tissues. In this paper, tangential forces that were not considered in the previous study [1] will also be considered. The main purpose of obtaining force information is to determine the softness of tissue; thus, static force is a focus of this paper. The measured force value is displayed on the monitor and superimposed on the image obtained by the endoscope. Feedback information is presented at the video rate; if the computing time is less than the video rate (10–30 [Hz]), then (image) processing can be adapted. Therefore, an endoscope and a force visualization technique that does not require any electrical components are used in this study. The target area of application is neurosurgery, such as an examination of tumors of the pituitary gland. For example, in examinations of tumors in the pituitary gland, the typical magnitude of force is around 0.1 [N] [15-17]. A resolution close to 0.01 [N] is then required [15-17]. To detect these small magnitudes at high resolution, highly elastic panty stocking fabric is used in the study.
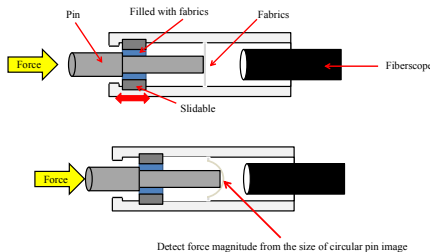
B. Force sensing principle

Figure 2. Principle for sensing force in depth direction of endoscope

1) Depth direction of endoscope:

The same principle as in the previous study [1] was considered. Fig. 2 shows a schematic diagram of the basic force sensing concept in the depth direction of endoscope. The force visualization part is attached to the tip of the fiberscope. If objects or tissues make contact with the pin and force is applied along the depth direction of the fiberscope (horizontal direction in Fig. 2), the pin slides in this direction and approaches the fiberscope. The pin is in contact with the elastic fabric shown in the middle area of Fig. 2 (Region A in Fig. 4). The distance traveled by the pin then depends on the magnitude of the applied/contact force. The elastic fabric plays the role of a spring. The image of the pin covered with the elastic fabric is captured by the fiberscope. The pin image becomes larger as the applied/contact force increases. The magnitude of the applied/contact force is then derived from the size of the pin image.
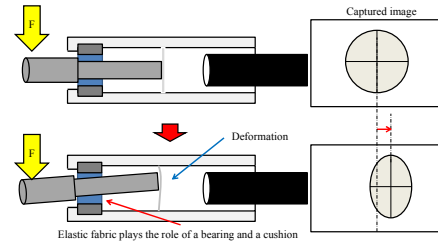

Figure 3. Principle for sensing force in directions tangential to tip surface

2) Direction tangential to tip surface:

Fig. 3 shows a schematic diagram of the basic force sensing concept in the directions tangential to tip surface (vertical direction in Fig. 3). The elastic part (blue area in Fig. 3 or region B in Fig. 4) was put in to connect the pin and the slider by fitting. The material of the elastic part is a highly elastic panty stocking fabric. This part serves as a bearing and cushion. If objects or tissues make contact with the pin and forces are applied along directions tangential to the tip surface, the pin tilts. Depending on the tilt, the pin image slides in the frame captured by the fiberscope. The sliding distance of the center position of the pin image corresponds to the distance traveled by the tip because of the force applied in the tangential direction. The magnitude of the applied/contact force is then derived from the sliding distance of the center position of the pin image. Note that the change of shape in the pin image also corresponds to the applied forces. However, the sliding distance of the center position was derived because it was easier.
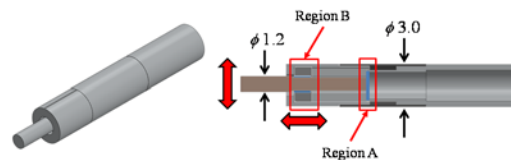

Figure 4. Overview of force visualization part

C. Structure of force visualization part

Fig. 4 shows the designed force visualization part. Its main components are the pin, fabric, fiberscope, and their connecting parts. A 20-denier panty stocking fabric, which plays the role of a spring, is installed at region A in Fig. 4.
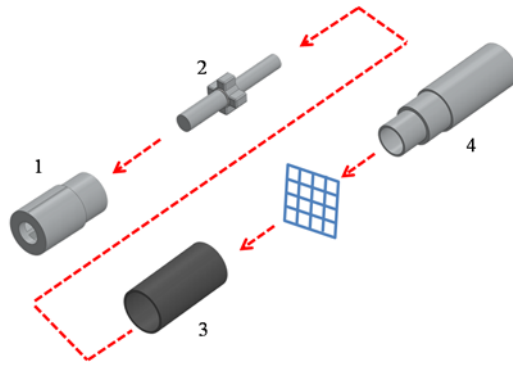
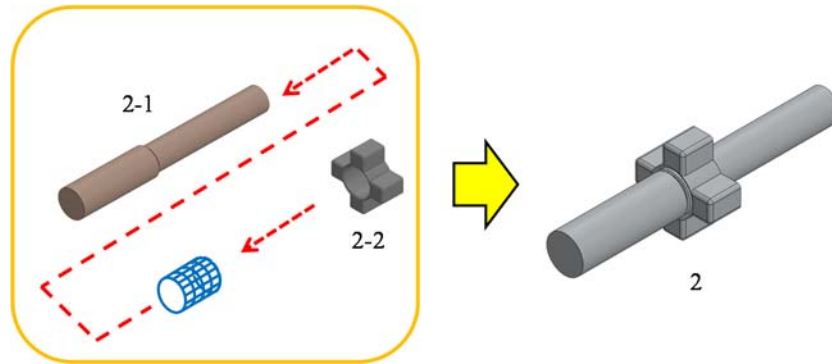Figure 5.   Overview of assembly process for force visualization part

Figure 6.   Overview of assembly process for pin (part 2 in Fig. 5)
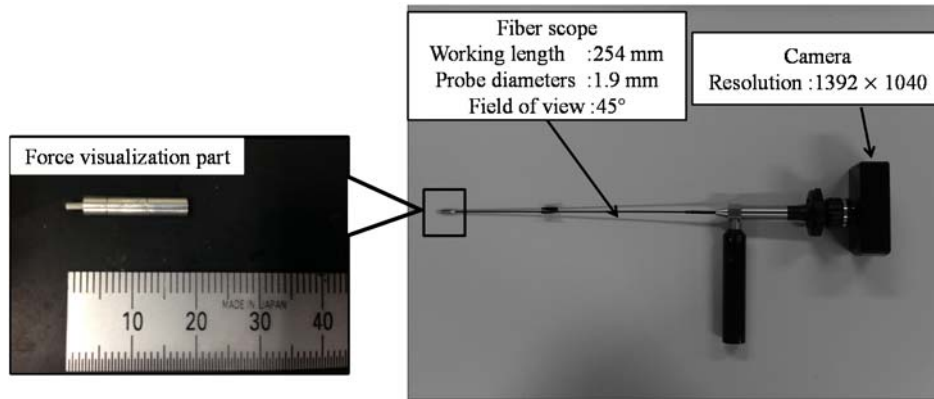

Figure 7.   Photograph of the manufactured force visualization part and a complete view of the developed force sensing system

TABLE I.   SPECIFICATIONS OF CAMERA (LUMENERA LU 135)

Size of image	1392 × 1040
Frame rate	15 [fps]
Exposure time	66 [ms]
Whole gain	2.0 [dB]

The same fabric is also installed at region B in Fig. 4. This fabric plays the role of a cushion and bearing. Fig. 5 shows an overview of the assembly process for the force visualization part. First, the fabric is used to cover part 4, and it is fixed by linking parts 3 and 4. Second, part 2 (pin) is connected to the linked part (the fabric and parts 3 and 4). Finally, part 1 is connected to the linked part (the fabric and parts 2, 3, and 4). Fig. 6 shows an overview of the assembly process of the pin (part 2). After covering the fabric on part 2-1, part 2-2 is connected to the linked part (the fabric and part 2-1). Parts 1-4 were connected by fitting. Fig. 7 shows a photograph of the manufactured force visualization part and complete view of the developed force sensing system. Except for the fabric, the material used for the visualization part was duralumin. The visualization part was 18.5 [mm] long in the maximally extended state and had a maximum diameter of 3 [mm]. The fiberscope is a Super Thin Flexible Borescope (MEDIT) with a diameter of 1.9 [mm], full length of 254 [mm], and visual field of 45[°]. The camera (Lumenera Corporation: Lu 135), whose specifications (measurement conditions) are listed in Table 1, is connected to the fiberscope. An image captured by using the Lu 135 can be directly sent to a PC via a USB cable. Note that the effect of distortion when bending the endoscope was investigated during the study and no change of intensity in the captured image was identified.

III. DERIVATION OF FORCE VALUE FROM CAPTURED IMAGE

This section describes how to derive the force value from the image captured by a fiberscope. The method for deriving force in the depth direction of the fiberscope is the same as the method presented in a previous paper [1]. The method for deriving forces in directions tangential to the tip surface is mainly described.

A. Forces in directions tangential to tip surface

As mentioned above, the force is derived based on the center position of the pin image captured by the fiberscope. To derive forces in directions tangential to the tip surfaces (vertical direction in Fig. 3), the center position of the pin image is first extracted. The magnitude of the force in a tangential direction is then derived from the distance traveled by the center position.

1) Extraction of center position of the pin image

Fig. 8 shows the procedure for extracting the pin area in the image captured by fiberscope. The original captured image is shown in Fig. 8 (a). The area surrounded by the relatively dark region is the area of the pin with the elastic fabric. The following steps show how to extract the center position of the pin image captured by the fiberscope. The process was implemented with Halcon (MVTech). The total computing time was less than 100 [ms].

1. Smoothing and edge enhancement: Smoothing and edge enhancement are performed to reduce noise and clarify the boundary of the pin area. The obtained image is shown in Fig. 8 (b).

2. Converting to a grayscale image: The (color) image is converted to a grayscale image as a preprocessing step for binarization. Fig. 8 (c) shows the obtained image.

3. Binarizing and selecting area: The grayscale image is binarized. By searching the region with the maximum area in the obtained binarized image, the pin area was determined. Fig. 8 (d) shows the obtained image.

4. Extracting the center position: By calculating the geometrical center of the obtained pin area, the center position is extracted.

(a) Original image   (b) Smoothing and edge enhancement

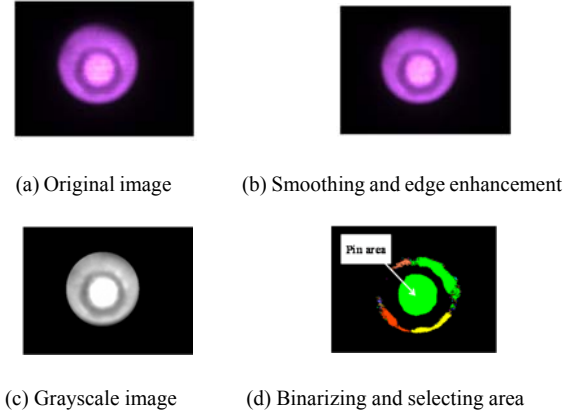(c) Grayscale image   (d) Binarizing and selecting area

Figure 8.   Procedure for extracting the pin area in the captured image
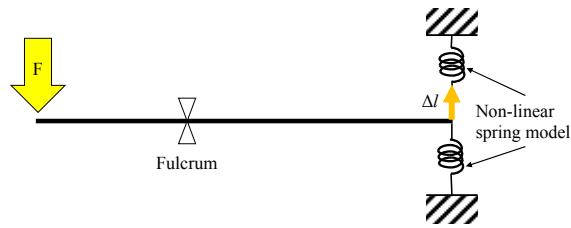

Figure 9.   Simplified model for derivation of forces in directions tangential to tip surface

2) Extraction of magnitude of force

The simplified model shown in Fig. 9 is considered to derive the value of the force. Because the center position of the pin image is used for the deviation, the pin is described as a line (whose right extreme point corresponds to the center position of the pin image) in this model. Note that the fabric also sits at the fulcrum, which corresponds to region B in Fig. 4. However, the effect of the fabric as a spring can be included in the non-linear spring model shown in Fig. 9. Therefore, the effect was ignored in this model. As experimentally demonstrated in a previous paper [1], the relationship between applied force and the moving distance of pin surface attached to the fabric (corresponding to Δl in Fig. 9; see also region A in Fig. 4) is considered to be nonlinear and is expressed by a polynomial function. In this paper, the relation is derived experimentally.

Fig. 10 shows the experimental setup for the investigation. The tip of the force visualization part is placed on the custom-made stage shown on the right side of Fig. 10. The custom-made stage is placed on the electronic weighting instrument (SHIMADZU TW223N), and the force applied to the stage in the vertical/downward direction is measured by the instrument. The force visualization part is attached to the fiberscope. Another custom-made stage linked to the automatic positioning stage (SIGMAKOKI SGSP15-10) is attached to the fiberscope to apply forces, as shown on the left side of Fig.

10. A force in a direction tangential to the tip surface (vertical direction in Figs. 3, 4, and 10) is applied by downwardly moving the automatic positioning stage.

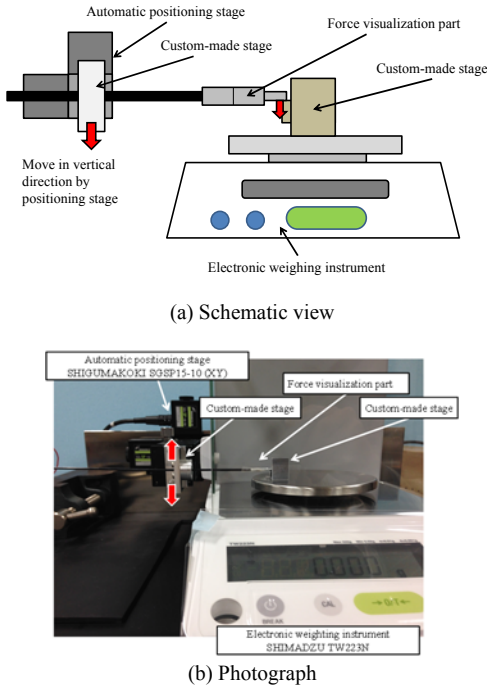(a) Schematic view

(b) Photograph

Figure 10. Experimental setup for investigating the relation between the applied force in direction tangential to the tip surface and the center position of the pin image

As the fundamental case, the force in the direction tangential to the tip surface was examined when the force in the depth direction of the fiberscope (horizontal direction in Fig. 10) was zero. The initial state is set such that the value shown by the electronic weighting instrument is 0.000 [g] while the pin of the force visualization part is in contact with the custom-made stage shown on the right side of Fig. 10. Subsequently, the automatic positioning stage was moved in steps of 100 [μm] to push the pin attached to the custom-made stage on the electronic weighting instrument until the total distance traveled reached 3.5 [mm] (The pin was moved 35 times). At each step, the applied force was measured by the electronic weighting instrument while the image was captured by the fiberscope. This procedure was repeated five times to confirm repeatability. Each measurement was conducted at 10-min intervals to minimize dynamic effects.
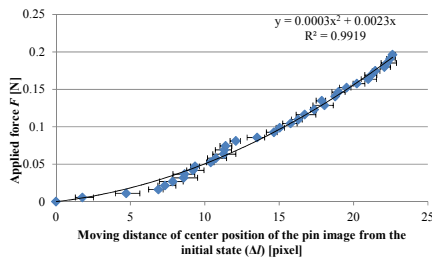

Figure 11. Relationship between the applied force F) in a direction tangential to the tip surface (vertical/downward direction in Fig, 10) and distance traveled by the center position of the pin image from the initial state (Δl).

Fig. 11 shows the experimental results for the relationship between the applied force (F) in a direction tangential to the tip surface (vertical/downward direction in Fig. 10) and the distance traveled by the center position of the pin image from the initial state (Δl). The diamond symbols indicate the measured points. The center position was derived by the method described in the previous subsection. A regression analysis was performed using the following third-order polynomial function

$$F = a\Delta l^2 + b\Delta l \tag{1}$$

where a and b were 0.30×10^{-3} [N/pixel^2] and 2.30×10^{-3} [N/pixel], respectively. The coefficient of determination was 0.99. The fitted curve expresses the relationship considerably well. Because (1) is a quadratic polynomial function, the resolution becomes lowest (i.e., 0.196 [N]) when the measured force value is highest. If the force value F is investigated so that the lowest Δl that produces 0.196 [N] exceeds the largest Δl that produces F, F turns out to be 0.18 [N]. The resolution is then better than 0.015 [N]. If the range that provides a resolution of more than 0.01 [N] is investigated, the range is 0–0.18 [N]. Therefore, the requirement of a resolution of more than 0.01 [N] is almost achieved.

Used (knitted) fabric has a reticular pattern and is manufactured using multiple (bended and twisted) strings. If the load is low, deformation of the fabric is mainly caused by stretching the bended strings. The relationship between load and displacement is then expressed by a nonlinear function [18], [19]. If the load is high, the strings are stretched, and the deformation is dominated by the stiffness of the strings themselves. In this case, the relationship between load and displacement is expressed by a linear function. In the study, the maximum applied force was roughly 0.20 [N] and the load was assumed to be low. In this case, a nonlinear function should be chosen for regression. Hence, a third-order polynomial function is used.

B. Force in the depth direction of fiberscope

The same method as that used in the previous study [1] was adapted. If the applied force in the depth direction of the fiberscope is large, the size of the pin image is also large. That is, the applied force is inversely related to the radius of the circular image of the pin. The relationship is expressed by the following a second-order polynomial function:

$$F_d = a_d\left(\frac{1}{r}\right)^2 + b_d\left(\frac{1}{r}\right) + c_d \tag{2}$$

where F_d is the applied force, r is the radius of the circular image of the pin, and a_d, b_d, and c_d are constants (see [1] for further details). This concrete relationship is experimentally examined in the developed system.

Fig. 12 shows a schematic view of the experimental setup for the investigation. Force0 was applied by a force gauge (IMADA ZP-5N, resolution: 0.001 [N]) attached to an automatic positioning stage (Oriental Motor ELSM2YF030-KD-C, movement speed: 100 [mm/s]). A pin attached to the tip of the force gauge was used to push the force visualization part attached to the fiberscope. The fiberscope was fixed to a custom-made stage so that the direction of pushing could be

controlled. The initial state was set such that the value shown by the force gauge was 0.000 [N] while both pins were in mutual contact. Then, the automatic positioning stage was moved in steps of 0.02 [N] to push the pin attached to the fiberscope until the applied force reached 0.2 [N]. At each step, the image was captured using the fiberscope. The procedure was repeated five times.
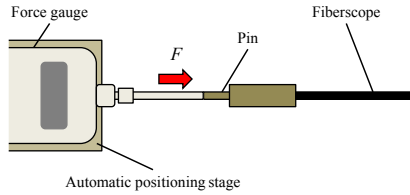

Figure 12. Schematic view of experimental setup for investigating the relationship between the applied force in depth direction of fiberscope and the inverse of the radius of the circular pin image
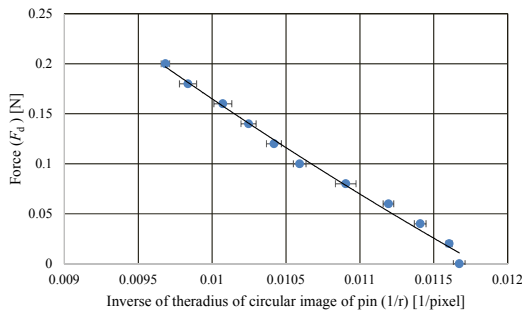

Figure 13. Relationship between the applied force in the depth direction of fiberscope (F_d) and the inverse of the radius of the circular pin image ($1/r$)

Fig. 13 shows the results. The radius of the circular pin image was calculated in the same manner as in a previous study [1]. Note that this is the same method as that described in section III.A.1 until step 3. At step 4, the radius was calculated instead of the center position. A regression analysis was performed using (2), and constant values of $a_d = 4.63 \times 10^3$, $b_d = -1.92 \times 10^2$, and $c_d = 1.63$ were obtained. The coefficient of determination was 0.99. The fitted curve expresses the relationship very well, and the resolution was better than 0.01 [N].

IV. CONCLUSION

A novel 3-axis force sensing system that could be attached to a fiberscope was presented in this paper. This system is an extension of our previous 1-axis force sensing system [1]. The main features are its compact size, high resolution, low cost, absence of electrical parts, and disposability. It was experimentally demonstrated that the system had a resolution of less than 0.01 [N].

There are several future directions for research. For use in the real world, a systematic calibration method that includes camera verification (so that the camera can capture a perfect image) is needed. Further, forces in the depth direction and tangential directions were separately investigated. In future work, forces in combined directions will be analyzed. Further, issues such as waterproofing and dynamic forces, which were beyond the scope of the present study, will also be

investigated.

REFERENCES

[1] T. Watanabe, T. Iwai, Y. Fujihira, L. Wakako, H. Kagawa and T. Yoneyama, "Force sensor attachable to thin fiberscopes/endoscopes utilizing high elastic fabric," *Sensors* (submitted) vol.14 pp.5207-5220.
[2] P. Puangmali, K. Althoefer, D. Seneviratne, D. Murphy, and P. Dasgupta, "State-of-the-art in force and tactile sensing for minimally invasive surgery," *Sensors Journal*, Vol. 8, No. 4, pp. 371–381, 2008.
[3] E. W. Van der Putten, R. Goossens, J. Jakimowicz, and J. Dankelman, "Haptics in minimally invasive surgery-a review," *Minimally Invasive Therapy & Allied Technologies*, Vol. 17, No. 1, pp. 3–16, 2008.
[4] A. Okamura, C. Verner, and M. Mahvash, "Haptics for robotassisted minimally invasive surgery," *Robotics Research*, 2011, pp. 361–372.
[5] E. V. Poorten, E. Demeester, and P. Lammertse, "Haptic feedback for medical applications, a survey," *Proceedings Actuator*, 2012, pp.18–20.
[6] M. I. Tiwana, S. J. Redmond, and N. H. Lovell, "A review of tactile sensing technologies with applications in biomedical engineering," *Sensors and Actuators A*, Vol. 179, pp. 17-31, 2012.
[7] T. Takaki, Y. Omasa, I. Ishii, T. Kawahara, and M. Okajima, "Force visualization mechanism using a moire fringe applied to endoscopic surgical instruments," *Proc. of IEEE Int. Conf. on Robotics and Automation*, 2010, pp. 3648–3653.
[8] K. Tadano and K. Kawashima, "Development of 4-dofs forceps with force sensing using pneumatic servo system," *Proc. of IEEE Int. Conf. on Robotics and Automation*, 2006, pp. 2250–2255.
[9] T. Kawahara, S. Tanaka, and M. Kaneko, "Non-contact stiffness imager," *Int. J. of Robotics Research*, Vol. 25, No. 5-6, pp.537–549, 2006.
[10] J. Peirs, J. Clijnen, D. Reynaerts, H. V. Brussel, P. Herijgers, B. Corteville, and S. Boone, "A micro optical force sensor for force feedback during minimally invasive robotic surgery," *Sensors and Actuators A*, Vol. 115, pp. 447-455, 2004.
[11] M. Tada, S. Sasaki, and T. Ogasawara, "Development of an optical 2-axis force sensor usable in MRI environments," *IEEE Sensors*, Vol. 2, pp. 984-989, 2002.
[12] M. Ohka, Y. Mitsuya, Y. Matsunaga, and S. Takeuchi, "Sensing characteristics of an optical three-axis tactile sensor under combined loading," *Robotica*, Vol. 22, No. 2, pp. 213-221, 2004.
[13] K. Kamiyama, K. Vlack, T. Mizota, H. Kajimoto, N. Kawakami, and S. Tachi, "Vision-based sensor for real-time measuring of surface traction fields," *IEEE Computer Graphics and Applications*, Vol. 25, Issue 1, pp. 68-75, 2005.
[14] R. S. Dahiya, G. Metta, M. Valle, and G. Sandini, "Tactile Sensing - From Humans to Humanoids," IEEE Trans. on Robotics. Vol. 6, Issue 1, pp. 1-20, 2010.
[15] T. Yoneyama, T. Watanabe, H. Kagawa, J. Hamada, Y. Hayashi, and M. Nakada, "Force-detecting gripper and force feedback system for neurosurgery applications," *Int. J. for Computer Assisted Radiology and Surgery*, 2013.
[16] Y. Kanada, T. Yoneyama, T. Watanabe, H. Kagawa, N. Sugiyama, K. Tanaka, and T. Hanyu, "Force feedback manipulating system for neurosurgery," *Procedia CIRP*, 2013. Vol. 5, pp. 133–136.
[17] Y. Fujihira, T. Hanyu, Y. Kanada, Y. Yoneyama, T. Watanabe, and H. Kagawa, "Gripping Force Feedback System for Neurosurgery," *Int. J. of Automation Technology*, Vol. 8, No. 1, pp. 83-94, 2014.
[18] S. Kawabata, "Linearizing Method" for Solving Non-linear Biaxial Tensile Property of fabric," *J. Text. Mach. Soc. Japan*, Vol. 39, No. 11, T169-T173, 1968.
[19] S. Kawabata, "A Method of Theoretical Calculation of Tensile Properties of Knitted Fabric from its Structure and Yarn Properties," *J. Text. Mach. Soc. Japan*, Vol. 23, No. 1/2, T30-T34, 1970.